



Published in final edited form as:

J Biomech. 2007 ; 40(15): 3516–3520. doi:10.1016/j.jbiomech.2007.04.019.

ACCURACY AND PRECISION OF DIGITAL VOLUME CORRELATION IN QUANTIFYING DISPLACEMENTS AND STRAINS IN TRABECULAR BONE

Li Liu and Elise F. Morgan

Abstract

Strain measurement is an essential tool in the study of trabecular bone structure-function relationships. Digital volume correlation (DVC) is a measurement technique that quantifies strains throughout the interior of a specimen, rather than simply those on the surface. DVC relies on tracking the movement of microstructural features, and as such, the accuracy and precision of this technique may depend on trabecular structure. This study quantified displacement and strain measurement errors in six types of trabecular bone that spanned a wide range of volume fraction and trabecular architecture. Accuracy and precision were compared across bone type and also across three DVC methods. Both simulated and real displacement fields were analyzed using micro-computed tomography images of specimens from the bovine distal femur, bovine proximal tibia, rabbit distal femur, rabbit proximal tibia, rabbit vertebra, and human vertebra. Differences as large as three-fold in accuracy and precision of the displacements and strains were found among DVC methods and among bone types. The displacement precision and the strain accuracy and precision were correlated with measures of trabecular structure such as structural model index. These results demonstrate that the performance of the DVC technique can depend on trabecular structure. Across all bone types, the displacement and strain errors ranged 1.86–3.39 μm and 345–794 $\mu\epsilon$, respectively. For specimens from the human vertebra and bovine distal femur, the measurement errors were approximately twenty times smaller than the yield strain. In these cases, DVC is a viable technique for measuring pre- and post-yield strains throughout trabecular bone specimens and the trabecular compartment of whole bones.

Keywords

cancellous bone; strain measurement; interior strains; whole bone; trabecular architecture

INTRODUCTION

Strain measurement is an essential tool in the study of bone structure-function relationships. Digital volume correlation (DVC) is potentially a powerful strain measurement technique for trabecular bone, because this technique can measure strains throughout the interior of a specimen. DVC is an extension of digital image correlation (Peters, 1982) that uses series of 3-D images, such as those provided by micro-computed tomography (μCT), to track the

Corresponding author: Elise F. Morgan, Boston University, 110 Cummington Street, Boston, MA 02215, p: (617) 353-2791, f: (617) 353-5866, e: efmorgan@bu.edu.

Publisher's Disclaimer: This is a PDF file of an unedited manuscript that has been accepted for publication. As a service to our customers we are providing this early version of the manuscript. The manuscript will undergo copyediting, typesetting, and review of the resulting proof before it is published in its final citable form. Please note that during the production process errors may be discovered which could affect the content, and all legal disclaimers that apply to the journal pertain.

movement of microstructural features throughout the specimen in response to an applied load (Bay, 2001; Bay, et al., 1999). Given the anatomic locations of trabecular bone in the skeleton, interior strain measurements are needed to define the mechanical demands to which trabecular bone is subjected *in situ*. If sufficiently accurate and precise, DVC could be used to measure, for the first time, the deformations that occur throughout the trabecular compartment of bones such as the vertebra and proximal femur during activities of daily living and during trauma. Such measurements are relevant for studies of whole bone failure mechanisms and bone adaptation.

The accuracy and precision of DVC have not yet been fully established. Previous studies have found that the displacement precision ranges 0.005–0.056 voxels and the strain precision ranges from tens to tens of thousands of microstrain depending on the length scale over which the strains are computed (Bay, et al., 1999; Verhulp, et al., 2004; Zael, et al., 2006). However, these previous studies have used one or two specimens only. The DVC technique is likely very sensitive to the nature of the trabecular structure, which would make the accuracy and precision vary depending on specimen density and trabecular architecture. Further, although different image correlation methods have been proposed (*e.g.*, Bay, et al., 1999; Huang, et al., 1997; Sutton, et al., 1983), no systematic comparison of their performance for trabecular bone has been reported. This study quantified the accuracy and precision of DVC across a wide range of trabecular structures in order to determine how the accuracy and precision vary with: 1) DVC method, and 2) trabecular structure.

METHODS

Specimens ($n=2$ /bone type) from the bovine distal femur (BDF), bovine proximal tibia (BPT), rabbit distal femur (RDF), rabbit proximal tibia (RPT), rabbit vertebral body (RVB), and human vertebral body (HVB) were imaged twice (36 μm /voxel resolution, 70 kVp, 300ms integration time; $\mu\text{CT}40$, Scanco Medical, Bassersdorf, Switzerland). A 4.3mm cubic image volume was selected from each specimen (Figure 1). Given the small size of the rabbit bones, inclusion of some of the cortical shell (RDF, RPT, RVB) and physis (RDF, RPT) was unavoidable. For these specimens, the results characterize DVC performance not for trabecular bone only but rather for regions of bone representative of those that would be analyzed when applying DVC to quantify deformations occurring throughout whole bones.

Performances of three DVC methods were compared: cross-correlation (CC) (Willert and Gharib, 1991); normalized cross-correlation (NCC) (Huang, et al., 1997); and maximum likelihood estimation (MLE) (Gokhale, et al., 2004). Details of these methods are provided as supplemental information on the journal website. Briefly, all three methods estimate the displacement field by matching sub-regions of two image volumes. Matching is performed by computing the similarity between the sub-regions' intensity (grayscale value) patterns. The CC and NCC methods use correlation functions as the similarity measure, and the MLE method uses the sum of the squared differences in intensities.

Both simulated and real displacement fields were analyzed. Simulated displacement fields were constructed from a *single* scan of a given specimen by translating the image volume by a uniform amount (2.0 or 0.5 voxels) in *each* coordinate direction (total displacement of 3.46 and 0.87 voxels, respectively). Accuracy and precision of the computed displacements were quantified by the mean and standard deviation, respectively, of the difference between the computed and true total displacements. To obtain a real, and ideally zero-valued, displacement field, the pair of scans for a given specimen was analyzed. Due to the finite precision of the μCT scanner stepper motor, the true displacement is not zero; thus, only the displacement precision, as quantified by the standard deviation, was evaluated for the case of repeated scans. Accuracy and precision of the strain were quantified by the mean and standard deviation,

respectively, of the average of the absolute values of the six strain components. All calculations were performed for four sub-region sizes: 20×20×20, 30×30×30, 40×40×40, and 50×50×50 voxels³.

Two-factor analyses of variance with Tukey *post hoc* tests were performed to identify differences in accuracy among DVC methods and among bone types (JMP 6.0, SAS Institute, Cary, NC). These analyses took into account that multiple sub-regions were analyzed for each specimen (nested, random effect) and that the displacement and strain for each sub-region were computed for each DVC method (repeated measures). Differences in precision were determined using Levene's test for homogeneity of variance. This test was performed separately for each method and bone type. The Dunn-Sidak method was used to account for multiple comparisons, resulting in a significance level (α) of 0.0052. Correlation analyses were performed to investigate the sensitivity of the displacement and strain errors to trabecular structure, as quantified by volume fraction, mean trabecular thickness, mean trabecular spacing, trabecular number, and structural model index.

RESULTS

The accuracy and precision of the displacements and strains differed among DVC methods (Table 1). For simulated displacements, the MLE method yielded the most accurate ($p < 0.001$) and precise ($p \leq 0.003$) displacement estimates. For the repeated scans, the displacement precision of the MLE and CC methods was higher ($p \leq 0.001$) than that of the NCC method for all bone types except the vertebral specimens. With respect to strains, the MLE method yielded the highest accuracy for all bone types ($p < 0.001$, Figure 2A) and highest precision for two bone types (RPT and RVB, $p < 0.003$, Figure 2B). No other differences in strain precision were found among methods ($p > 0.05$). In all cases, the error magnitudes decreased with increasing sub-region size.

The displacement and strain errors also differed among bone types (Table 1). For simulated displacements, differences in displacement accuracy among bone types differed depending on DVC method ($p < 0.001$); however, the precision was highest for the bovine and human specimens for all methods ($p \leq 0.001$). For the repeated scans, the displacement precision was highest for the bovine distal femur for all methods ($p < 0.001$). The strain accuracy was highest for the human vertebra and bovine distal femur and lowest for the rabbit distal femur and rabbit proximal tibia ($p < 0.001$, Figure 2A). No differences in strain precision among bone types were found ($p > 0.02$, Figure 2B); however, the accuracy and precision were highest for specimens with lower volume fraction and trabecular number, and higher trabecular spacing and structural model index (Table 2).

DISCUSSION

When both accuracy and precision of the displacements and strains are considered, the MLE method demonstrated the best performance. For this method, the displacement precision ranged 1.86–3.39 μm (0.052–0.094 voxels) and the strain errors ranged 345–794 $\mu\epsilon$ across all bone types for a sub-region size of 40 voxels. Under the stipulation that a strain measurement technique can reliably measure strains equal to or greater than ten times the error, the MLE method can measure strains as small as approximately half the yield strain ($\sim 7000 \mu\epsilon$ (Morgan and Keaveny, 2001)) in some bone types (*e.g.* HVB, BDF). Thus, in some cases DVC is a viable technique for quantifying pre- and post-yield strains in the trabecular compartment of whole bones. However, the variability in performance among bone types and DVC methods suggest that as a general rule, applications of DVC may be restricted to the yield and post-yield regimes.

There are several limitations of this study. First, analyses were conducted only on images of undeformed samples; thus, strain decorrelation was not considered (Westerweel, 1997). Second, not all specimens consisted exclusively of trabecular bone (Figure 1). We believe that the large errors obtained for the rabbit tibia and femur were due to the physis, which appears as a region of low intensity variations in the μ CT images. Third, only one image resolution was investigated. However, an ancillary analysis of image resolution (Table 3) indicates that small differences in resolution do not affect displacement precision.

The levels of precision found here are comparable to those in previous DVC studies on μ CT images of trabecular bone (Bay, et al., 1999; Zauel, et al., 2006) when differences in subregion size are considered. They are also comparable to those reported for ultrasonic imaging (Chen, et al., 1992; Ophir, et al., 2001); however, they are four to ten times lower than those reported for optical imaging (Cheng, et al., 2002; Chevalier, et al., 2001; Nicoletta, et al., 2006; Nicoletta, et al., 2001; Pitter, et al., 2002; Tong, 1997; Zhang, et al., 2003) and approximately ten times higher than those reported for magnetic resonance imaging (Bey, et al., 2002; Gilchrist, et al., 2004). These differences may result from differences among these studies in imaging modalities, in technical approaches, and in image texture (Gilchrist, et al., 2004) of the various specimens. The results of this study highlight the importance of the latter by indicating that differences in structure among specimens can affect the accuracy and precision of the estimated deformations.

Supplementary Material

Refer to Web version on PubMed Central for supplementary material.

Acknowledgements

Funding for this study was provided in part by an unrestricted grant from the International Osteoporosis Foundation and Servier. Human tissue was obtained from the National Disease Research Interchange. The authors would also like to thank Paul Barbone for many helpful discussions on digital image correlation and displacement estimation.

References

- Bay BK. Experimental measurement of three-dimensional continuum-level strain fields in trabecular bone. *Adv Exp Med Biol* 2001;496:181–97. [PubMed: 11783619]
- Bay BK, Smith TS, Fyhrie DP, Saad M. Digital volume correlation: three-dimensional strain mapping using x-ray tomography. *Experimental Mechanics* 1999;39:217–26.
- Bey MJ, Song HK, Wehrli FW, Soslowsky LJ. A noncontact, nondestructive method for quantifying intratissue deformations and strains. *J Biomech Eng* 2002;124:253–8. [PubMed: 12002136]
- Bruck HA, McNeill SR, Sutton MA, Peters WH. Digital Image Correlation using Newton-Raphson Method of Partial Differential Correction. *Experimental Mechanics* 1989;29:261–7.
- Chen, EJ.; Jenkins, WK.; O'Brien, WD, Jr. The accuracy and precision of estimating tissue displacements from ultrasonic images; Tucson, AZ, USA. 1992.
- Cheng P, Sutton MA, Schreier HW, McNeill SR. Full-field speckle pattern image correlation with B-spline deformation function. *Experimental Mechanics* 2002;42:344–52.
- Chevalier L, Calloch S, Hild F, Marco Y. Digital image correlation used to analyze the multiaxial behavior of rubber-like materials. *European Journal of Mechanics, A/Solids* 2001;20:169–87.
- Gilchrist CL, Xia JQ, Setton LA, Hsu EW. High-resolution determination of soft tissue deformations using MRI and first-order texture correlation. *IEEE Trans Med Imaging* 2004;23:546–53. [PubMed: 15147008]
- Gokhale N, Richards M, Oberai A, Barbone P. Simultaneous elastic image registration and elastic modulus reconstruction. *IEEE International Symposium on Biomedical Imaging* 2004;1:543–6.
- Huang H, Dabiri D, Gharib M. On errors of digital particle image velocimetry. *Measurement Science and Technology* 1997;8:1427–40.

- Morgan EF, Keaveny TM. Dependence of yield strain of human trabecular bone on anatomic site. *Journal of Biomechanics* 2001;34:569–77. [PubMed: 11311697]
- Nicoletta DP, Moravits DE, Gale AM, Bonewald LF, Lankford J. Osteocyte lacunae tissue strain in cortical bone. *J Biomech* 2006;39:1735–43. [PubMed: 15993413]
- Nicoletta DP, Nicholls AE, Lankford J, Davy DT. Machine vision photogrammetry: a technique for measurement of microstructural strain in cortical bone. *Journal of Biomechanics* 2001;34:135–9. [PubMed: 11425075]
- Ophir J, Kallel F, Varghese T, Konofagou E, Alam SK, Krouskop T, Garra B, Righetti R. Elastography. *Comptes Rendus de l'Academie des Sciences, Serie IV (Physique, Astrophysique)* 2001;2:1193–212.
- Peters WH, Ranson WF. Digital imaging techniques in experimental stress analysis. *Optical Engineering* 1982;21:427–31.
- Pitter MC, See CW, Goh JYL, Somekh MG. Focus errors and their correction in microscopic deformation analysis using correlation. *Optics Express* 2002;10:1361–7.
- Schreier HW, Brassch JR, Sutton MA. Systematic errors in digital image correlation caused by intensity interpolation. *Optical Engineering* 2000;39:2915–21.
- Sutton MA, McNeill SR, Jinseng J, Majid B. Effects of subpixel image restoration on digital correlation error estimates. *Optical Engineering* 1988;27:870–7.
- Sutton MA, Wolters WJ, Peters WH, Ranson WF, McNeill SR. Determination of displacements using an improved digital correlation method. *Image and Vision Computing* 1983;1:133–9.
- Tong W. Detection of plastic deformation patterns in a binary aluminum alloy. *Experimental Mechanics* 1997;37:452–9.
- Verhulp E, van Rietbergen B, Huiskes R. A three-dimensional digital image correlation technique for strain measurements in microstructures. *J Biomech* 2004;37:1313–20. [PubMed: 15275838]
- Westerweel J. Fundamental of digital particle image velocimetry. *Measurement Science and Technology* 1997;8:1379–92.
- Willert CE, Gharib M. Digital particle image velocimetry. *Experimental in Fluids* 1991;10:181–93.
- Zael R, Yeni YN, Bay BK, Dong XN, Fyhrie DP. Comparison of the linear finite element prediction of deformation and strain of human cancellous bone to 3D digital volume correlation measurement. *Journal of Biomechanical Engineering* 2006;128:1–6. [PubMed: 16532610]
- Zhang J, Jin G, Ma S, Meng L. Application of an improved subpixel registration algorithm on digital speckle correlation measurement. *Optics and Laser Technology* 2003;35:533–42.

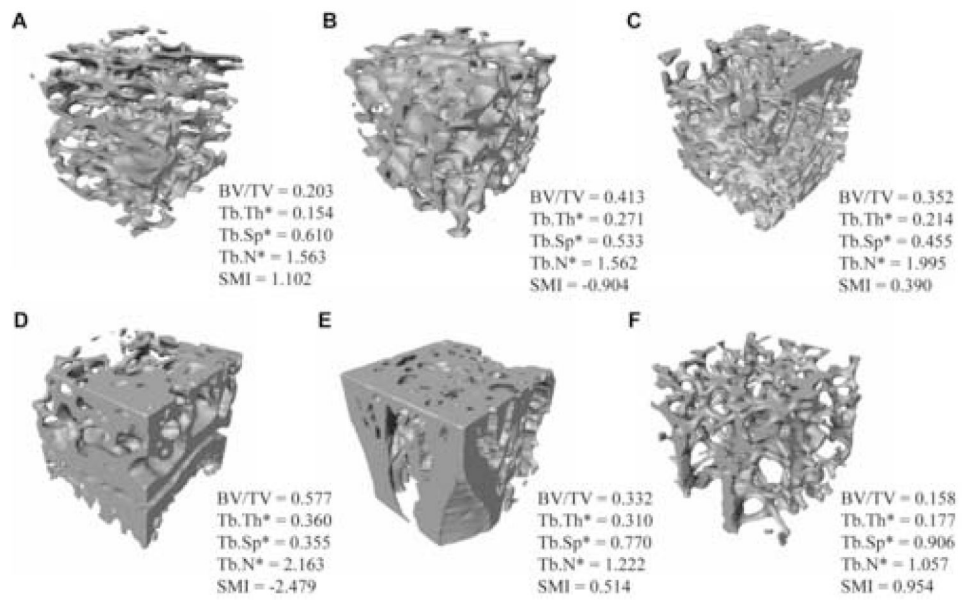
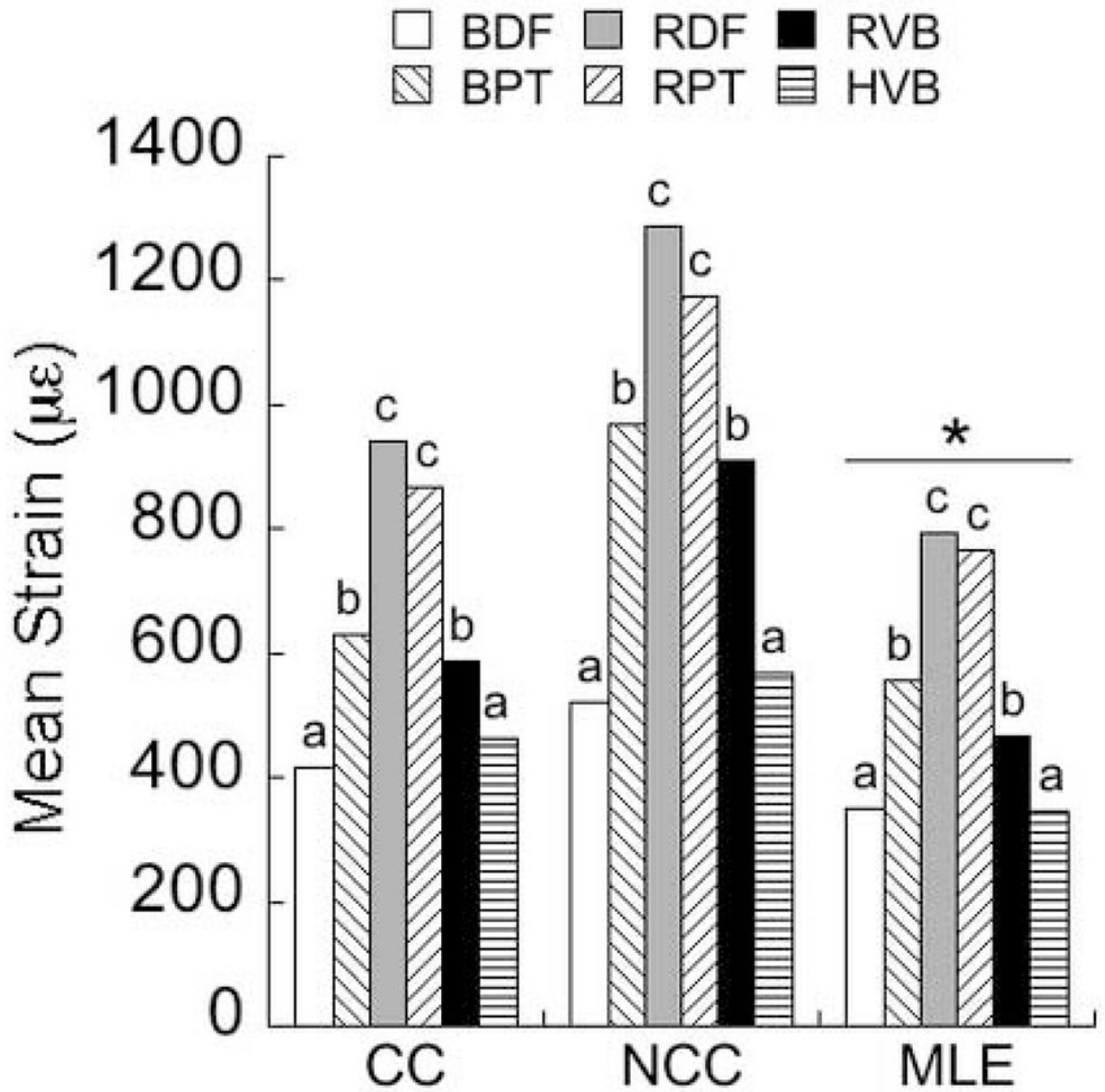


Figure 1.

A



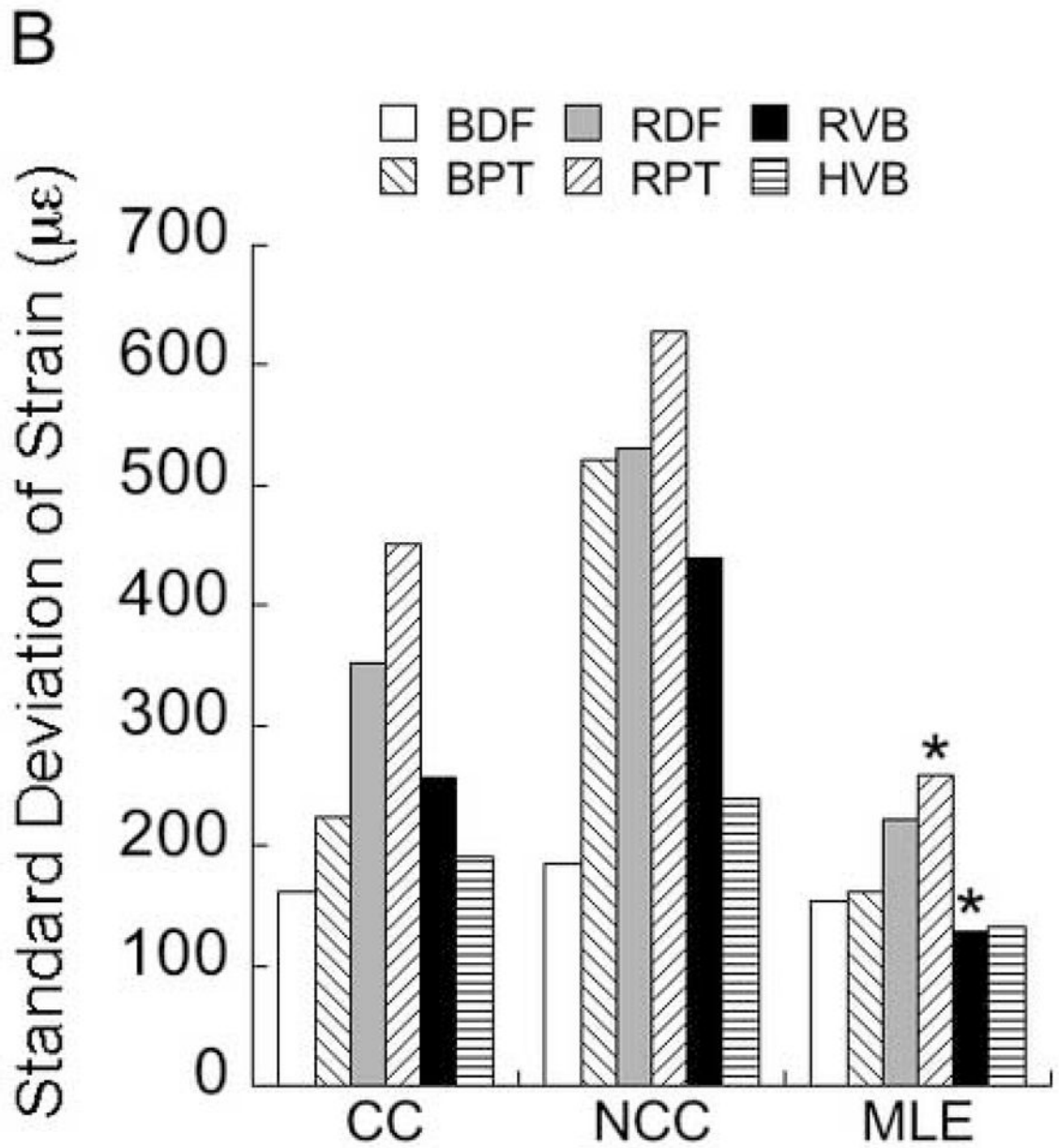


Figure 2.

Table 1

	CC		NCC		MLE	
	(μm)	(Voxel)	(μm)	(Voxel)	(μm)	(Voxel)
BDF						
Mean1	-5.53 ^c	-0.154 ^c	2.02 ^b	0.056 ^c	0.08	0.002
STD1 ⁺	2.34	0.065	3.05 ^{**}	0.085 [*]	2.47	0.069
STD2 ⁺⁺	1.87	0.052	2.38 ^{**}	0.066 ^{**}	1.86	0.052
BPT						
Mean1	-14.70 ^d	-0.408 ^a	-8.31 ^d	-0.231 ^d	-0.01	0.000
STD1 ⁺	1.81	0.050	2.59 [*]	0.072 [*]	1.67	0.046
STD2	3.27	0.091	5.79 ^{**}	0.161 ^{**}	2.52	0.071
RDF						
Mean1	-7.20 ^c	-0.200 ^c	0.88 ^b	0.025 ^b	-0.18	-0.005
STD1	4.11	0.114	5.07 ^{**}	0.141 ^{**}	4.00	0.111
STD2	3.04	0.084	3.85 ^{**}	0.107 ^{**}	2.76	0.077
RPT						
Mean1	-10.05 ^b	-0.279 ^b	0.90 ^b	0.025 ^b	-0.19	-0.005
STD1	3.47	0.096	5.15 [*]	0.143 [*]	3.57	0.099
STD2	3.49	0.097	4.96 ^{**}	0.138 ^{**}	3.39	0.094
RVB						
Mean1	-11.63 ^b	-0.323 ^b	0.44 ^b	0.012 ^b	-0.68	-0.019
STD1	4.92	0.137	6.01	0.167	5.05	0.140
STD2	2.62	0.073	3.68	0.102	2.62	0.073
HVB						
Mean1	-9.58 ^b	-0.266 ^b	-0.08 ^b	-0.002 ^b	0.16	0.004
STD1 ⁺	2.50	0.069	3.04 [*]	0.084 [*]	2.61	0.072
STD2	2.70	0.075	3.35	0.093	2.75	0.076

* Higher STD1 as compared to the other two DVC methods for a given bone type ($p \leq 0.003$)

** Higher STD2 as compared to the other two DVC methods for a given bone type ($p \leq 0.001$)

a, b, c. For a given DVC method, Mean1 values not labeled with the same letter are different from one another ($p < 0.001$)

⁺ Lower STD1 as compared to the other bone types for all three DVC methods ($p < 0.001$)

⁺⁺ Lower STD2 as compared to the other bone types for all three DVC methods ($p < 0.001$)

Table 2

	Displacement		Strain	
	STD _{CC}	STD _{MLE}	Mean _{CC}	STD _{CC}
BV/TV	0.58	0.54	0.69	0.76
Tb.Th*	0.49	0.50	0.47	0.64
Tb.Sp*	-0.30	-0.22	-0.63	-0.59
Tb.N*	0.28	0.25	0.66	0.67
SMI	-0.62	-0.59	-0.62	-0.70
			Mean _{MLE}	STD _{MLE}
			0.76	0.65
			0.51	0.44
			-0.74	-0.64
			0.75	0.69
			-0.69	-0.66

Table 3

Image Resolution ($\mu\text{m}/\text{voxel}$)	CC		MLE	
	(μm)	(Voxel)	(μm)	(Voxel)
20	1.20	0.060	1.22	0.061
36	2.32	0.064	2.47	0.069